


 Cite this: *RSC Adv.*, 2021, **11**, 33814

# Synthesis and functional studies of self-adjuvanting multicomponent anti-HER2 cancer vaccines†

 Qi Feng,<sup>a</sup> Xiaoyue Yu,<sup>be</sup> Yixue Wang,<sup>acde</sup> Shiyang Li<sup>acde</sup> and Yang Yang<sup>af</sup>

Breast cancer is the leading cause of cancer-related deaths among women worldwide. Human epidermal growth factor receptor 2 (HER2) overexpression is significantly associated with higher breast tumor proliferation rates. MFCH401, a 9-mer specific peptide fragment (DTILWKDIF) in the extracellular domain of the HER2 protein, is an attractive epitope for developing anti-HER2 cancer vaccines. However, the inherent low immunogenicity of MFCH401 limits its application. Herein, to induce a stronger and more durable immune response, a self-adjuvanting MFCH401-conjugated multiple-component anti-HER2 cancer vaccine was designed and synthesized by incorporating MFCH401 with lipopeptide Pam<sub>3</sub>CSK<sub>4</sub> and a helper T cell epitope derived from tetanus toxoid P2 *via* an iterative condensation reaction. *In vivo* immunological evaluation demonstrated that the tricomponent anti-HER2 vaccine induced stronger humoral and cellular immune responses than the two-component conjugates. In addition, the induced antibodies effectively bound to HER2-overexpressing human BT474 cells. Our data clearly indicated that the MFCH401-based tricomponent anti-HER2 cancer vaccine could effectively enhance the immunogenicity of MFCH401. Structure–activity relationship analysis demonstrated that Pam<sub>3</sub>CSK<sub>4</sub> confers better immunostimulatory activity than the helper T cell epitope P2 when conjugated with MFCH401.

 Received 16th August 2021  
 Accepted 23rd September 2021

DOI: 10.1039/d1ra06146a

[rsc.li/rsc-advances](http://rsc.li/rsc-advances)

## 1. Introduction

More than one million new cases of breast cancer are diagnosed annually and it is considered the leading cause of global female mortality.<sup>1</sup> Overexpression of human epidermal growth factor receptor 2 (HER2) has been reported to play a key role in the development of breast cancer and occurs in approximately 30% of breast cancer patients.<sup>2</sup> HER2 is a tumor-associated antigen (TAA) and is an important therapeutic target for breast cancer.<sup>3</sup> During the past few decades, clinical and basic research progress in the field of HER2-positive breast cancer therapy has improved remarkably.<sup>4</sup> Passive immunotherapy with recombinant monoclonal antibodies (mAbs) and related antibody drugs, particularly trastuzumab and pertuzumab, have been

widely used for the treatment of HER2-positive breast cancer.<sup>5</sup> However, drug resistance to mAbs therapy and occasional recurrence in clinical applications are still considered important challenges that cannot be ignored.<sup>6</sup> Recently, the development of active immunization with cancer vaccines has become an attractive strategy to replace traditional mAb-based passive immunotherapy, as it could prevent the occasional recurrence of cancer that results from drug resistance.<sup>7</sup> Currently, HER2-derived peptide fragments have been widely used to develop anti-HER2 peptide vaccines, such as E75, GP2, and AE37, and have been proven effective and safe in early phase clinical trials.<sup>8</sup> MFCH401 (DTILWKDIF), a 9-mer peptide derived from the extracellular domain of the HER2 protein, is demonstrated to be a promising epitope for the design of novel peptide vaccines.<sup>9</sup> However, the inherent poor immunogenicity and metabolic instability limit the development of peptide-based cancer vaccines.<sup>10</sup> To overcome these shortcomings, self-adjuvanting vaccine design strategies have become an attractive approach. Self-adjuvanting cancer vaccines are constructed by conjugating TAA with adjuvants that can easily break the immunotolerance and enhance the immunogenicity of conjugated antigens.<sup>11</sup> A precise synthetic self-adjuvanting vaccine with a well-defined structure could allow for a deeper understanding of the structure–activity relationship as well as easier quality control.<sup>12</sup>

Toll-like receptor (TLR) agonists are important activators of innate immune responses and are widely considered promising vaccine adjuvants.<sup>13</sup> TLR2 agonists, including diacylated

<sup>a</sup>Department of Nephrology, The First Affiliated Hospital of Zhengzhou University, Zhengzhou 450052, P. R. China. E-mail: fengqi2019@zzu.edu.cn

<sup>b</sup>Research Institute of Nephrology, Zhengzhou University, Zhengzhou 450052, P. R. China

<sup>c</sup>Henan Province Research Center For Kidney Disease, Zhengzhou 450052, P. R. China

<sup>d</sup>Key Laboratory of Precision Diagnosis and Treatment for Chronic Kidney Disease in Henan Province, Zhengzhou 450052, P. R. China

<sup>e</sup>Department of Cardiovascular Medicine, The First Affiliated Hospital of Zhengzhou University, Zhengzhou 450052, P. R. China

<sup>f</sup>Clinical Systems Biology Laboratories, The First Affiliated Hospital of Zhengzhou University, Zhengzhou, 450052, P. R. China. E-mail: yangyangbio@163.com

† Electronic supplementary information (ESI) available: A detailed description of the synthesis procedures of all compounds. See DOI: 10.1039/d1ra06146a



lipopeptides and triacylated lipopeptides derived from bacterial lipoproteins, play pivotal roles in inducing innate immune responses and modulating adaptive immune responses. During the past few years, they have been used as safe adjuvants and possess satisfactory immunological potential.<sup>14</sup> Among them, triacylated lipopeptide Pam<sub>3</sub>CSK<sub>4</sub> (TLR2/1 agonist) is the most widely employed built-in adjuvant for self-adjuvanting cancer vaccines.<sup>15</sup> Pam<sub>3</sub>CSK<sub>4</sub>-conjugated vaccines improve antigen presentation efficiency, protect antigens from enzymatic degradation, and induce the production of Th1 cytokines by activating TLR2/1.<sup>16–20</sup> Previously, we constructed a two-component conjugate MFCH401-Pam<sub>3</sub>CSK<sub>4</sub> as a potential anti-HER2 cancer vaccine, and *in vivo* immunological evaluation demonstrated that it could induce relatively higher IgG2b and IgG3 levels, which indicated a robust Th1 type immune response.<sup>9</sup>

In general, therapeutic cancer vaccines should be able to induce strong antitumor T-cell immune responses to directly kill cancer cells, and appropriate helper T cell epitopes are quite important for stimulating a strong antitumor effect by inducing a cell immune response.<sup>21</sup> For example, Boons *et al.* firstly constructed a tricomponent vaccine composed of the MUC1 antigen, lipopeptide Pam<sub>3</sub>CSK<sub>4</sub>, and a helper T cell epitope of poliovirus; *in vivo* immunological evaluation demonstrated that the tripartite vaccine elicited a robust IgG antibody response and exhibited superior antitumor effects compared to those of two-component vaccines.<sup>22</sup> Payne *et al.* constructed tricomponent vaccines by incorporating the MUC1 glycopeptide antigen with Pam<sub>3</sub>CysSer or Pam<sub>3</sub>CysSer and a peptide from tetanus toxin as a helper T cell epitope *via* iterative condensation reactions. *In vivo* immunological examination demonstrated that these vaccines elicited higher IgG antibody titers in mice.<sup>23</sup> Li and Kunz *et al.* synthesized a tricomponent vaccine containing the MUC1 antigen, lipopeptide Pam<sub>3</sub>CSK<sub>4</sub>, and a helper T cell epitope P2 (QYIKANSKFIGITE) of tetanus toxoid, which also displayed stronger immune responses than two-component vaccines.<sup>24</sup> Zhao *et al.* designed and synthesized a MUC1-based tricomponent vaccine by conjugating MUC1 antigen, a helper T cell epitope P2 (QYIKANSKFIGITE) with lipopeptide FSL-1, and the glycosylated tricomponent vaccine candidate enabled to induce the efficient elicitation of both humoral and cellular immune responses.<sup>25</sup> These studies provided strong evidence to support the design of multicomponent cancer vaccines.

In this study, to enhance the immune response effects of MFCH401-based anti-HER2 cancer vaccines, on the basis of two-component conjugate MFCH401-Pam<sub>3</sub>CSK<sub>4</sub>, we designed and synthesized tricomponent cancer vaccine candidate 1, which was composed of MFCH401 connected to the immunostimulant Pam<sub>3</sub>CSK<sub>4</sub> and a helper T cell epitope through covalent bonds. P2 (QYIKANSKFIGITE) derived from tetanus toxoid was introduced as a helper T cell epitope, and low-immunological triethylene glycolic acid was used as a linker to combine these three components. In addition, to explore the effect of the helper T cell epitope and immunoadjuvant Pam<sub>3</sub>-CSK<sub>4</sub> on the immunogenicity of MCH401, compound 3 containing MFCH401 and helper T cell epitope P2 (QYIKANSKFIGITE) was designed and prepared, and compound 2 was prepared as a control (Fig. 1).

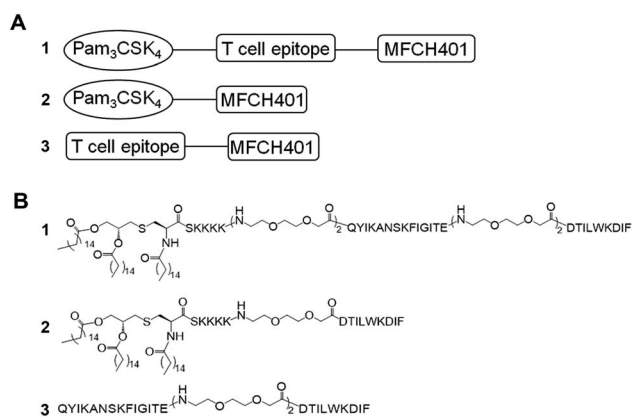


Fig. 1 Two- and three-component anti-HER2 vaccines that contain the MFCH401 epitope. The diagrams (A) and chemical structures (B) of vaccine candidates 1–3.

## 2. Materials and methods

### Materials and instruments

All commercial chemicals and biological reagents were purchased from commercial sources. The solvents used were reagent grade or HPLC grade. Matrix-assisted laser desorption/ionization time-of-flight mass spectrometry (MALDI-TOF MS) was performed using an UltrafleXtreme MALDI-TOF/TOF (Bruker, Germany). ESI-MS spectra were obtained using a Thermo Scientific LTQ Orbitrap XL™ spectrometer. Reversed-phase high-performance liquid chromatography (RP-HPLC) analysis was performed using a Shimadzu HPLC LC-20A. Enzyme-linked immunosorbent assay (ELISA) was performed to determine the cytokine expression levels using an uncoated ELISA kit with plates (Thermo Fisher). Corning® 96-well ELISA plates (9018, polystyrene) were used for ELISA detection of antibodies. Mouse IgG isotypes (IgG1, IgG2a, IgG2b, and IgG3) were purchased from Abcam. HER2 overexpressing BT474 cell lines were purchased from Cell Bank of Shanghai, Chinese Academy of Sciences (Shanghai, China). Flow cytometry was performed using a BD Accuri™ C6 Flow Cytometer.

### Vaccination schedule

All animal experiments in this study were conducted at the Experimental Animal Center of Zhengzhou University. Male Balb/c mice (6–8 weeks old) were housed in an SPF grade animal facility and maintained on a 12 h light/dark cycle with free access to water and food. Five male Balb/c mice in each group received an intraperitoneal injection of 3.5 nmol vaccine in 100 μL PBS on day 1, and three subsequent booster shots administered biweekly on days 16, 30, and 44. Mouse sera were collected *via* the tail vein one day prior to the initial immunization (day 0) and after immunization on days 9, 21, 35, and 49.

All animal procedures were performed in accordance with the Guidelines for Care and Use of Laboratory Animals of Zhengzhou University and approved by the Animal Ethics Committee of Zhengzhou University.



### ELISA for antibody titer analysis

The MFCH401-immobilized bovine serum albumin (BSA-MFCH401) conjugate was prepared using a thiol-based ligation strategy, as described in our previous report. In this study, 100  $\mu\text{L}$  BSA-MFCH401 ( $10 \mu\text{g mL}^{-1}$  in 0.05 M carbonate coating buffer, pH 9.5) was added to 96 well plates (Corning® 9018). After incubation at 4 °C overnight, the plates were washed three times with >250  $\mu\text{L}$  per well PBS washing buffer (pH 7.4). Subsequently, the plates were blocked with 2% BSA in carbonate coating buffer (pH 9.6) for 2 h at 37 °C. After washing three times, diluted mouse serum samples were added to the wells. After 2 h incubation, the plates were washed four times with >250  $\mu\text{L}$  of 0.5% Tween-20 in PBS, and then horseradish peroxidase (HRP)-conjugated goat anti-mouse IgG (Sigma, 100  $\mu\text{L}$  per well, 1000-fold dilution), IgM (Abcam, 100  $\mu\text{L}$  per well, 1000-fold dilution), IgG1, IgG2a, IgG2b, and IgG3 (Abcam, 100  $\mu\text{L}$  per well, 3000-fold dilution) were separately added to the plates. After 1 h incubation at room temperature, the plate was washed eight times with >250  $\mu\text{L}$  0.5% Tween-20 in PBS. The color reaction was performed by adding 100  $\mu\text{L}$  of an *O*-phenylenediamine dihydrochloride (OPD, Sigma) solution to each well. After incubation for 15–30 min, the color reaction was quenched with 2.5 M  $\text{H}_2\text{SO}_4$  (50  $\mu\text{L}$  per well) and the optical density of the formed dye was measured using a microreader at a wavelength of 492 nm and using a reference wavelength of 620 nm. The endpoints were considered to be  $A_{492} - A_{620} \leq 0.100$ .

### Cytokine analysis

The cytokine release levels in pre-immunized mice sera (day 0) and antisera immunized by 1, 2 and 3 (day 49) were measured four times using a mouse cytokine uncoated ELISA Kit (eBioscience, Ready-SET-Go!). Collected mice sera (day 0 and day 49) were diluted 1 : 2. Finally, the optical density of the formed dye was measured using a microreader at a wavelength of 450 nm, and the data were used as indexes of relative expression levels.

### Cell culture

Human breast cancer BT474 cells (HER2-overexpression) were cultured in RPMI1640 supplemented with 10% FBS and 1% antibiotics (penicillin/streptomycin), in 5%  $\text{CO}_2$  atmosphere at 37 °C.

### Flow cytometry analysis

BT474 cells were digested with 0.25% trypsin in EDTA solution and washed two times with cell culture medium, and then counted (cell count not less than  $1 \times 10^6$ ). Then, the suspension was centrifuged at 1500 rpm for 5 min to remove the medium. After washing twice with PBS buffer, 4% paraformaldehyde in PBS (500  $\mu\text{L}$ ) was added to each 1.5 mL tube containing washed cells. Then, the tubes were incubated at 37 °C for 10 min, followed by 1 min on ice for fixation. After fixation,  $5 \times 10^5$  cells were transferred to a 1.5 mL tube, and washed twice with FACS buffer. Furthermore, a suspension containing  $5 \times 10^5$  cells in 98  $\mu\text{L}$  FACS buffer was added to 2  $\mu\text{L}$  of mouse serum before immunization (day 0) and mouse serum after immunization

(day 49). After incubation at 4 °C for 1 h, the suspension was centrifuged at 2000 rpm for 5 min to remove the supernatant. After 3 times washing, cells were treated with a solution of Alex488-conjugated goat anti-mouse IgG (H + L) cross-adsorbed secondary antibody (1 : 50 dilution). After incubation at 4 °C for 30 min, the suspension was centrifuged at 2000 rpm (1820 g) for 5 min to remove the supernatant. After three washes, the cells were suspended in 500  $\mu\text{L}$  FACS buffer for flow cytometry analysis.

### Complement-dependent cytotoxicity (CDC) assay

The CDC directed towards BT474 cells recognized by the antibodies induced by synthetic anti-HER2 vaccine candidates 1, 2 and 3 was determined by using the tetrazolium bromide (MTT) test. BT474 cells ( $1 \times 10^4$  cells per well) were incubated with 100  $\mu\text{L}$  of diluted antisera in PBS buffer (v/v = 1 : 5). After washing, rabbit sera diluted in DMEM medium (v/v = 1 : 5) were used as the complement supplier. Rabbit complement (RC) was inactivated by treatment at 65 °C for 30 min (without the incubation of any sera) and was presented as 100% cell viability (RC-inactive). The cytotoxicity of the rabbit complement itself was also evaluated (RC). The cell viability was measured after incubation with complement for 2 h.

### Statistical analysis

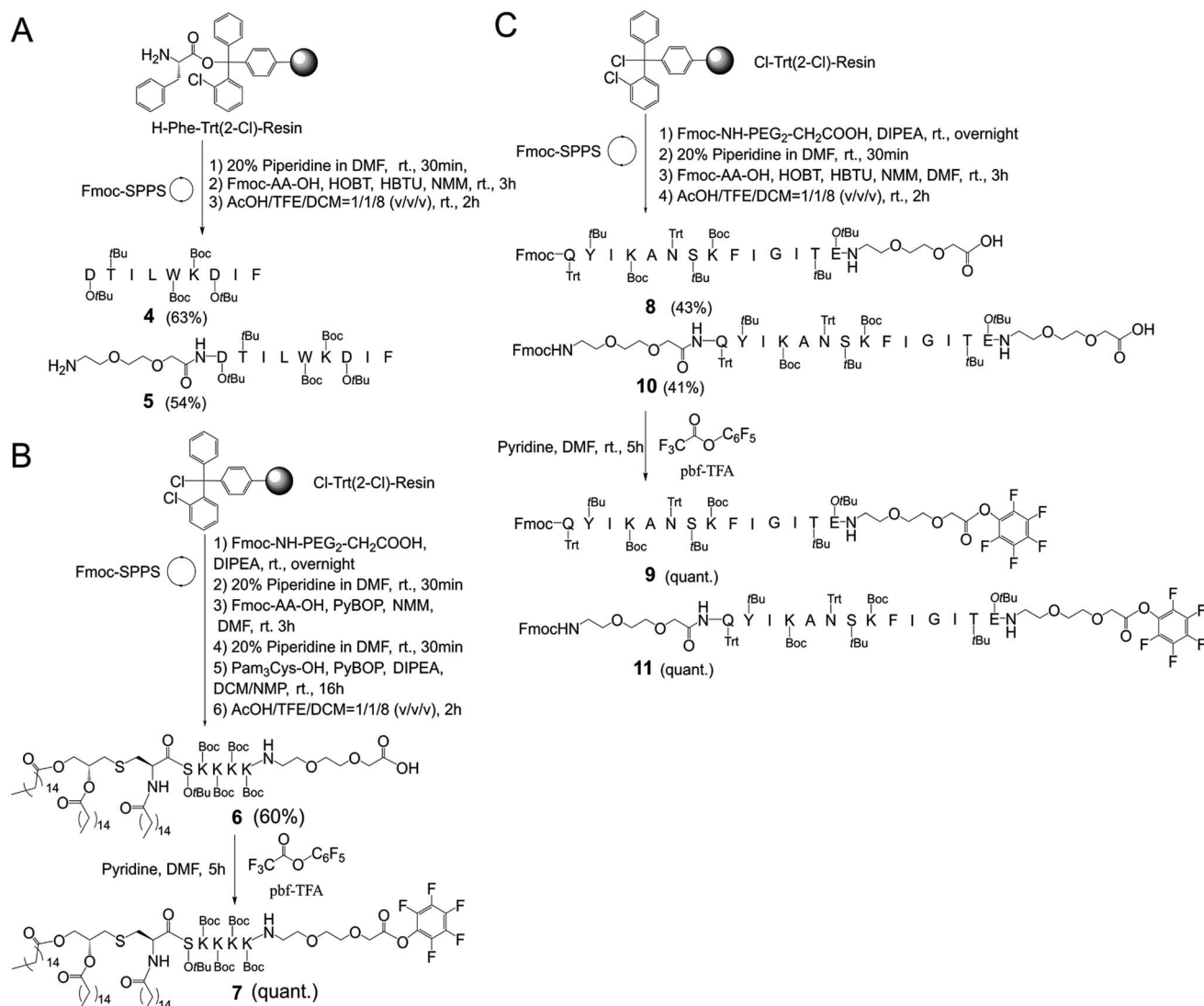
Data is expressed as the mean  $\pm$  standard deviation (SD). Statistical analysis was performed using SPSS 17.0 software, assuming a significance level of  $p < 0.05$ . Student's *t*-test was used to assess the statistical significance between the different experimental groups. \* indicates  $p < 0.05$ , \*\* indicates  $p < 0.01$ , \*\*\* indicates  $p < 0.01$ .

## 3. Results

### Chemical synthesis

In this study, it firstly needs to prepare the key intermediates on an appropriate scale as they are the basic structural fragments for preparing MFCH401-based anti-HER2 vaccine candidates, 1, 2, and 3 (Scheme 1). The synthesis started with the preparation of side-chain protected compounds 4, 5, 6, 8 and 10 through Fmoc solid-phase peptide synthesis (Fmoc-SPPS). Compound 4 and 5 were synthesized by loading Fmoc-Ile-OH on 2-chlorotrityl chloride resin preloaded with phenylalanine in the presence of *O*-(1*H*-benzotriazol-1-yl)-*N,N,N',N'*-tetramethyluronium hexafluoro-phosphate (HBTU)/1-hydroxybenzotriazole (HOBt) and *N*-methylmorpholine (DMM) in dimethylformamide (DMF). Then, Fmoc was removed with 20% piperidine in DMF, and the coupling reaction of Fmoc-protected amino acids (Fmoc-AA-OH) or Fmoc-protected triethylene glycolic acid (Fmoc-PEG<sub>2</sub>-CH<sub>2</sub>COOH) was performed to give resin-linked peptides. Subsequently, the Fmoc protection group was removed with 20% piperidine in DMF, and the side chain protected peptide 4 (63% in yield) and 5 (54% in yield) were afforded by using acetic acid (AcOH)/tetrafluoroethanol (TFE)/dichloromethane (DCM) (v/v/v = 1 : 1 : 8), respectively (Scheme 1A). Similarly, compounds 8 and 10 were also prepared



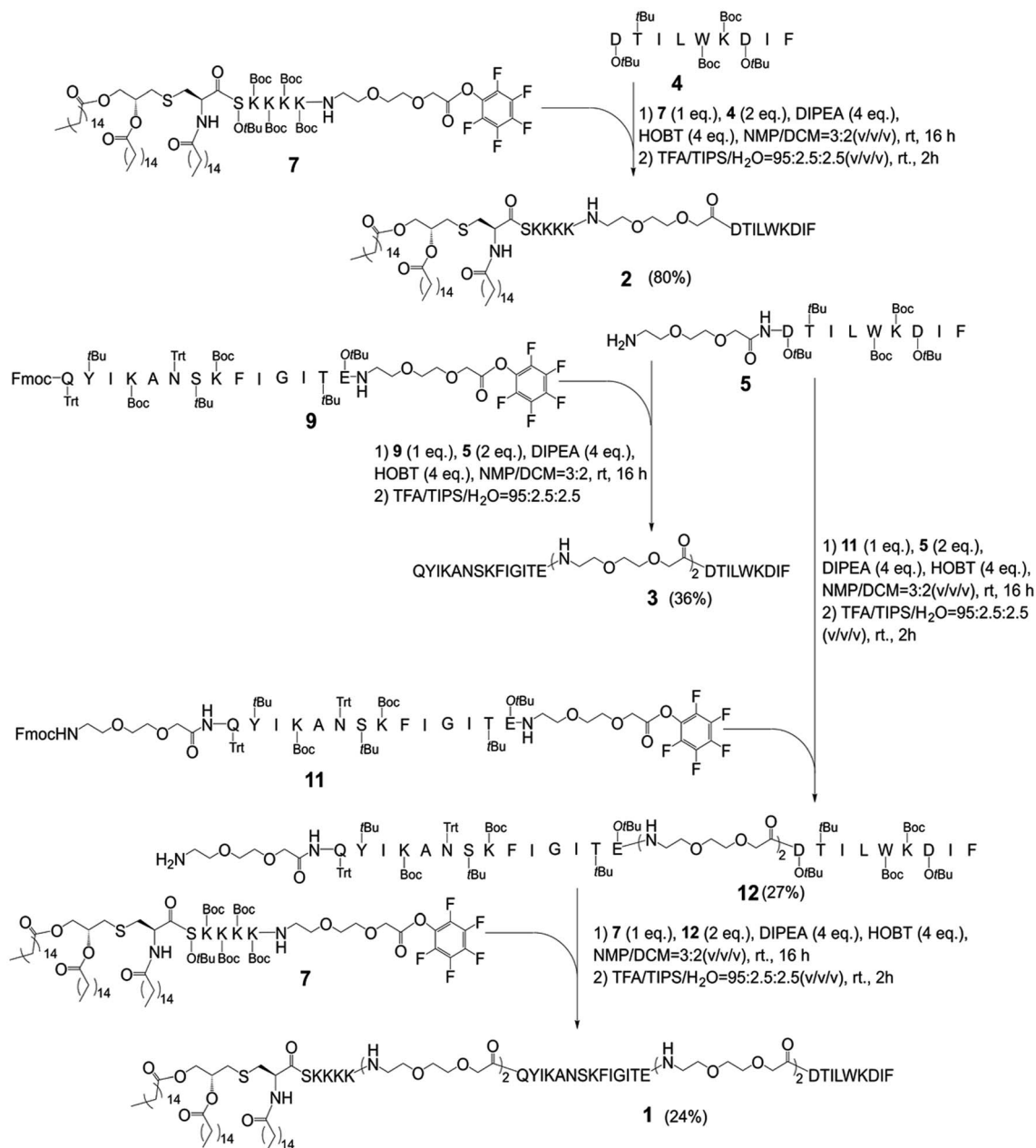


Scheme 1 Synthesis of the key intermediates 4 and 5 (A), 6 and 7 (B) and 8–11 (C).

via Fmoc-SPPS, which started with the introduction of Fmoc-PEG<sub>2</sub>-CH<sub>2</sub>COOH on 2-chlorotrityl chloride resin in the presence of diisopropylethylamine (DIPEA) in DMF/DCM (v/v = 1 : 1). After Fmoc removal and elongating the peptide chain by coupling of the Fmoc-AA-OH or Fmoc-PEG<sub>2</sub>-CH<sub>2</sub>COOH, the resin-bound peptides were afforded. Then, the side-chain protected compounds **8** and **10** were detached from the resin by using AcOH/TFE/DCM (v/v/v = 1 : 1 : 8) and purified by silica gel column chromatography in excellent yields (43% and 41%, respectively). Finally, compounds **6** and **8** were separately treated with pentafluorophenol trifluoroacetate (pbf-TFA) and pyridine in the presence of DMF to afford the active pentafluorophenol esters **9** and **11** in a quantitative yield (Scheme 1C). Additionally, compound **6** was prepared according to a previously reported method<sup>9</sup>(see ESI<sup>†</sup>), and subsequently activated by pbf-TFA to afford the active pentafluorophenol esters **7** (Scheme 1B). After affording the key intermediates (Scheme 1), the pentafluorophenyl ester-mediated fragment

condensation reaction between **5** and **9** or **11** was carried out in the selected solvent system NMP/DCM (3 : 2) to afford vaccine candidates **3** and compound **12** in excellent yields (36% and 27%, respectively) after purification by RP-HPLC. Besides, compound **7** was reacted with **4** in the presence of HOBT and DIPEA under the solvent system NMP/DCM (3 : 2), followed by global deprotection by using trifluoroacetic acid (TFA)/triisopropylsilane (TIS)/H<sub>2</sub>O (v/v/v = 95 : 2.5 : 2.5) to afford vaccine candidate **2** (80% in yield). Similarly, the conjugation of **7** and **12** was successfully carried out in the solvent system NMP/DCM (3 : 2) containing DIPEA and HOBT. Finally, all side chain protective groups were removed using 95% TFA, 2.5% TIPS, and 2.5% H<sub>2</sub>O. After purification by RP-HPLC on a semi-preparative C4 column, we obtained target compound **1** (24%) in higher yield (Scheme 2). In addition, based on our previous study, BSA-MFCH401 and linker-immobilized BSA (BSA-linker) were prepared *via* thiol-reactive group-based ligation and used as coating substrates for ELISA.<sup>9</sup>





Scheme 2 The syntheses of anti-HER2 vaccine candidates 1–3.

### Immunological evaluation

BALB/c mice were used to evaluate the immunostimulatory activity of vaccine candidates 1–3. Female BALB/c mice (five mice per group) were divided into four groups, including a control group and three vaccination groups. Each mouse in the control group was immunized with 100  $\mu$ L of phosphate-buffered saline (PBS). The mice in the vaccination groups received immunizations on day 1, followed by three bi-weekly boosters on days 16, 30, and 44 *via* intraperitoneal injection with 4 nmol vaccine dissolved in 100  $\mu$ L sterile PBS solution (see ESI<sup>†</sup>). After finishing the vaccination schedule, sera were collected one day prior to the initial immunization on day 0 (blank control) and on days 9, 21, 35, and 49. Subsequently,

ELISA was performed to evaluate MFCH401-specific antibody titers in collected sera, and BSA-MFCH401 and BSA-linker were used as coating substrates (see ESI<sup>†</sup>).

As shown in Fig. 2, the titers of MFCH401-specific IgG and IgM antibodies induced by tricomponent vaccine candidate 1 elicited higher IgG and IgM titers than those induced by two-component vaccine candidates 2 and 3, indicating that the tricomponent vaccine could induce robust antigenic responses compared to the two-component vaccines. It also supported both immunoadjuvant and helper T cell epitopes are necessary for the efficient production of IgG antibodies. Compared with vaccine candidate 3, vaccine candidate 2 induced high IgG and IgM antibody titers, suggesting that the covalent attachment of



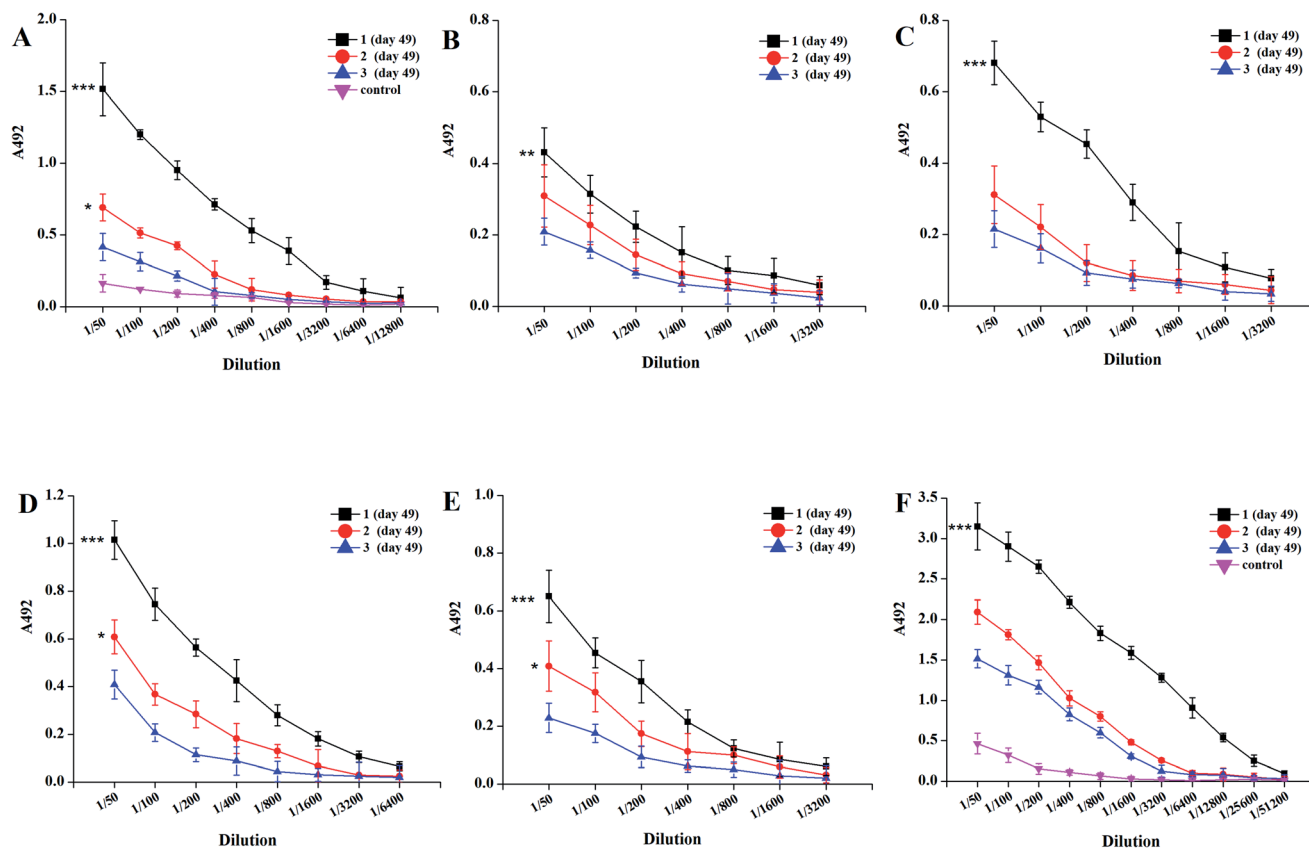


Fig. 2 The ELISA results of mice antisera antibody titers after immunization by vaccine candidates 1–3. (A) IgG, (B) IgG1, (C) IgG2a, (D) IgG2b, (E) IgG3 and (F) IgM. Mice were immunized biweekly for four times, and the sera collected on day 49 were assessed by MFCH401-specific-ELISA. ELISA plates were coated with BSA-MFCH401 according to reported methods. The sera collected before immunization were used as control. \*\*\* $P < 0.001$  vs. 3, \*\* $P < 0.01$  vs. 3, \* $P < 0.05$  vs. 3.

MFCH401 to immunoadjuvant Pam<sub>3</sub>CSK<sub>4</sub> conferred higher immune stimulation potential than the covalent linkage of MFCH401 to helper T cell epitope P2. In addition, vaccine candidates 1–3 induced the production of IgG and IgM antibodies against BSA, and the BSA-PEG linker was very low, indicating the weaker antigenicity of the PEG linker used in this study.

Subsequently, we examined the antibody titers of the different IgG subclasses. The IgG1 subclass antibody reflects the effect of a Th2-type immune response, and IgG2a/2b/3 subclass antibodies represent the effect of Th1-type immune response.<sup>26</sup> Tricomponent vaccine 1 elicited high levels of IgG1, IgG2a, and IgG2b antibodies, indicating that 1 could induce mixed Th1/Th2 responses. To further investigate the status of immune responses induced by synthetic vaccine candidates, we measured the cytokine release in collected antisera. After four immunization cycles, the expression levels of TNF- $\alpha$ , IL-6, IL-4, and IL-10 were increased, especially in the vaccine 1 immunization group, indicating the activation of Th1, Th2, and NK cells (Fig. 3). Therefore, vaccine candidate 1 not only induced robust humoral immune responses but also elicited Th1 and Th2 cell-mediated cellular immune responses. These results reveal that the conjugate of MFCH401 with the immunoadjuvant Pam<sub>3</sub>-CSK<sub>4</sub> and helper T cell epitope is critical for inducing robust immune responses.

In this study, the binding affinity of IgG antibody in anti-sera induced by designed vaccines 1–3 to BT474 (HER2 high expression) human breast cancer cells was examined by flow cytometry (FACS) analysis. The results demonstrated that IgG

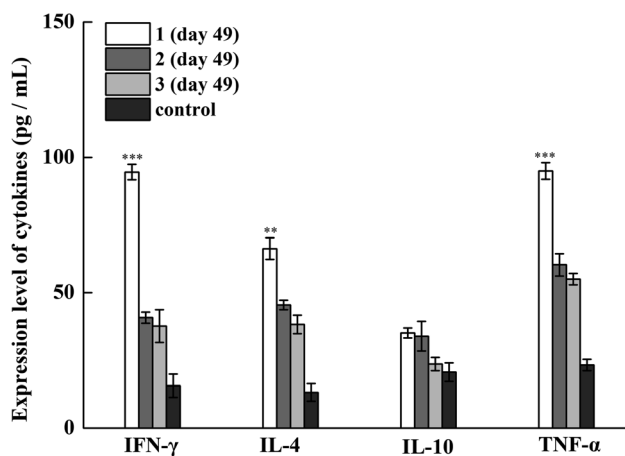


Fig. 3 The expression levels of IFN- $\gamma$ , IL-4, IL-10 and TNF- $\alpha$  in the pre-immune mouse sera (control) and the day 49 antisera from mice immunized with vaccine candidates 1–3. \*\*\* $P < 0.001$  vs. 3, \*\* $P < 0.01$  vs. 3.



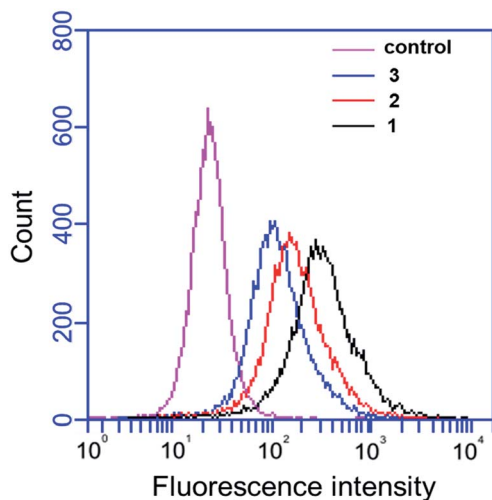


Fig. 4 Flow cytometry analysis of the binding affinity of induced antisera to HER2 high expression cancer cells. Alexa Fluor@488-goat anti-mouse IgG was used for staining. The binding of vaccine candidates 1–3 immunized antisera with BT474. The antisera induced by 1 was shown in black, the antisera induced by 2 was shown in red, and the antisera induced by 3 was shown in blue. The sera from pre-immune mice were used as control (pink).

antibodies induced by vaccines 1–3 could easily recognize high-expressing HER2 BT474 cells, which demonstrates that self-adjuvanting two- and tricomponent vaccines based on MFCH401 can elicit effective IgG antibody immune responses. Compared with vaccine 2, we found that vaccine 1 induced IgG antibody exhibited a higher affinity for binding BT474 cells, indicating that the helper T cell epitope P2 was important for the efficient production of the IgG antibody. In addition, the IgG antibodies in antisera induced by tricomponent vaccine 1 exhibited a higher binding affinity for BT474 cells compared with two-component vaccines 2 and 3 elicited IgG antibodies. This suggests that both immunoadjuvant Pam<sub>3</sub>CSK<sub>4</sub> and the helper T cell epitope are necessary for the efficient production of IgG antibodies, which is consistent with the ELISA results described previously (Fig. 4).

The antitumor activities against HER2 overexpressing BT474 cells mediated by antisera that induced by the synthetic anti-HER2 vaccines 1, 2 and 3 were evaluated through activation of the complement-dependent cytotoxicity (CDC)<sup>27</sup> (Fig. 5). As depicted in Fig. 5, the tetrazolium bromide (MTT) assays of the survival rate indicated the killing rates of BT474 cells mediated by anti-1, anti-2 and anti-3 sera were about 22%, 40% and 54%, respectively. When compared to the control group, the results strongly confirmed that the antisera raised by vaccine 1, 2 and 3 mediated effective and specific CDC to cancer cells which overexpressing HER2 antigen. Additionally, the data further demonstrated that vaccine 1 induced antisera mediated strongest CDC activity against BT474 cells than anti-sera stimulated by vaccine 2 and vaccine 3, moreover anti-2 sera mediated significantly better CDC activity to BT474 cells than anti-3 sera under the same condition. The above results supported that vaccine 1 was a better vaccine than 2 and 3 for cancer immunotherapy.

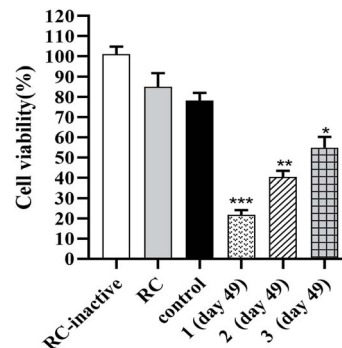


Fig. 5 The results of antibody-mediated complement-dependent cytotoxicity to BT474 cells. RC-inactive: the cell viability of inactivated rabbit complement is taken as 100% cell viability; RC: rabbit complement; control denotes the mouse sera before immunization; 1 (day 49), 2 (day 49) and 3 (day 49) denotes the day 49 antisera from mice immunized with vaccine candidates 1, 2 and 3. Data shown are the mean of three independent experiments. \*\*\* $P < 0.001$  vs. control, \*\* $P < 0.01$  vs. control, \* $P < 0.05$  vs. control.

## 4. Discussion

Currently, active immunotherapy with cancer vaccines is a popular strategy for treating various cancers.<sup>28</sup> Previously, to break the immune tolerance and overcome the low immunogenicity of MFCH401, two-component anti-HER2 cancer vaccines containing MFCH401 or its linear tandem repeats and lipopeptide Pam<sub>3</sub>CSK<sub>4</sub> were designed and synthesized.<sup>9</sup> The biological study demonstrated that MFCH401 is a promising epitope for breast cancer vaccine design, and a self-adjuvanting strategy could significantly improve the immunogenicity of MFCH401. Previously, to improve the intensity of immune responses of two-component MUC1-conjugated vaccines, Li and colleagues designed and synthesized tricomponent glyco lipopeptide vaccines and induced high production of IgG1, IgG2a, IgG2b, and IgG3 antibodies in mice. Moreover, the immunological evaluation exhibited a significant upregulation of the IgG2a/IgG1 ratio and an enhanced cytotoxic effect.<sup>24</sup>

In this study, we also successfully afford a self-adjuvanting tricomponent anti-HER2 cancer vaccine 1 for the first time, containing the MFCH401 epitope, immunoadjuvant Pam<sub>3</sub>CSK<sub>4</sub>, and a helper T cell epitope P2. Simultaneously, two-component vaccine candidates 2 and 3 were synthesized as controls, to further explore their structure–activity relationship. Immunological evaluation revealed that tricomponent vaccine 1 elicited robust IgG and IgM immune responses than the other vaccine conjugates. Moreover, cytokine release studies demonstrated that the expression levels of IL-6, IL-4, IL-10, and TNF- $\alpha$  in mice serum from the vaccine 1 immunization group were higher than those in other groups, suggesting that Th1 and Th2 immunity was effectively induced by vaccine 1. Additionally, FACS analysis demonstrated that the IgG antibodies induced by vaccines 1–3 could effectively recognize HER2 over-expressing BT474 cells. In particular, tricomponent vaccine 1 exhibited a higher binding affinity to BT474 cells than two-component vaccine candidates 2 and 3, confirming that both immunoadjuvant Pam<sub>3</sub>CSK<sub>4</sub> and helper T cell epitope P2 are necessary for the efficient production of HER2-targeting IgG



antibody. Likewise, antibody-mediated CDC assay also indicated that the anti-1 sera could mediate strongest killing rate against HER2 overexpressing BT474 breast cancer cells than anti-sera stimulated by vaccine 2 and vaccine 3 under the same conditions, which supported the similar results in previous studies.<sup>20,23–25</sup>

Furthermore, tricomponent vaccine 1 with its simple lipopeptide adjuvant-helper T cell epitope P2-minimal epitope conjugated structure also exhibited Th1 and Th2-skewed responses, which strongly supported the self-adjuvanting vaccine strategy with multiple components. In addition, the *in vivo* results also indicated that immunoadjuvant Pam<sub>3</sub>CSK<sub>4</sub> could stimulate a stronger immune response than the helper T cell epitope. Therefore, we greatly believe that lipopeptide-conjugated tricomponent vaccine 1 is a promising vaccine candidate in cancer immunotherapy for further clinical applications.

## 5. Conclusion

Combinations of lipopeptide Pam<sub>3</sub>CSK<sub>4</sub>, HER2-derived peptide epitope MFCH401, and helper T cell epitope P2 were used to construct two- and tricomponent anti-HER2 cancer vaccines using an iterative condensation reaction method. The *in vivo* immunological evaluation results showed that the antibody induced by tricomponent MFCH401-conjugated vaccine 1 not only significantly recognized and bound HER2-overexpressing BT474 breast cancer cells, but also effectively initiated the killing of the recognized BT474 cells through activation of the complement-dependent cytotoxicity, which strongly indicated tricomponent vaccine 1 possessed higher antitumor immune response potential than that of two-component vaccine candidates 2 and 3. More importantly, the applied multivalent vaccine design strategy worked as expected. Therefore, all of the above results have demonstrated that MFCH40-conjugated multivalent vaccine is a better choice than the self-adjuvanting two-component conjugate under experimental conditions, and our study provides important information for the further design and optimization of anti-HER2 cancer vaccines, which is worth further investigation and development.

## Author contributions

Qi Feng designed this study, performed the experiments, organized and analyzed the data, and wrote draft manuscript. Xiaoyue Yu and Yixue Wang conducted the animal experiments. Shiyang Li contributed to make suggestions for revision. Yang Yang contributed to review the manuscript and analyze the data. All authors had read and agreed to the published version of the manuscript.

## Conflicts of interest

The authors declare no conflict of interest.

## Acknowledgements

This work was financially supported in part by Key R&D and promotion Special Projects of Henan Province (No. 212102310194), Joint construction project of Henan Medical

Science and technology research plan in 2019 (No. LHGJ20190265) and Initial Scientific Research Fund of Young Teachers in Zhengzhou University (No. 32211235).

## References

- 1 M. Solanki and D. Visscher, *Hum Pathol*, 2020, **95**, 137–148.
- 2 M. G. Cesca, L. Vian, S. Cristovao-Ferreira, N. Ponde and E. de Azambuja, *Cancer Treat Rev*, 2020, **88**, 102033.
- 3 A. Arab, R. Yazdian-Robati and J. Behravan, *Arch Immunol Ther Exp*, 2020, **68**, 2.
- 4 E. Krasniqi, G. Barchiesi, L. Pizzuti, M. Mazzotta, A. Venuti, M. Maugeri-Sacca, G. Sanguineti, G. Massimiani, D. Sergi, S. Carpano, P. Marchetti, S. Tomao, T. Gamucci, R. De Maria, F. Tomao, C. Natoli, N. Tinari, G. Ciliberto, M. Barba and P. Vici, *J Hematol Oncol*, 2019, **12**, 111.
- 5 R. K. Murthy, S. Loi, A. Okines, E. Paplomata, E. Hamilton, S. A. Hurvitz, N. U. Lin, V. Borges, V. Abramson, C. Anders, P. L. Bedard, M. Oliveira, E. Jakobsen, T. Bachelot, S. S. Shachar, V. Muller, S. Braga, F. P. Duhoux, R. Greil, D. Cameron, L. A. Carey, G. Curigliano, K. Gelmon, G. Hortobagyi, I. Krop, S. Loibl, M. Pegram, D. Slamon, M. C. Palanca-Wessels, L. Walker, W. Feng and E. P. Winer, *N. Engl. J. Med.*, 2020, **382**, 597–609.
- 6 F. W. Hunter, H. R. Barker, B. Lipert, F. Rothe, G. Gebhart, M. J. Piccart-Gebhart, C. Sotiriou and S. M. F. Jamieson, *Br. J. Cancer*, 2020, **122**, 603–612.
- 7 U. Sahin and O. Tureci, *Science*, 2018, **359**, 1355–1360.
- 8 G. T. Clifton, E. A. Mittendorf and G. E. Peoples, *Immunotherapy*, 2015, **7**, 1159–1168.
- 9 Q. Feng, Y. Manabe, K. Kabayama, T. Aiga, A. Miyamoto, S. Ohshima, Y. Kametani and K. Fukase, *Chem Asian J*, 2019, **14**, 4268–4273.
- 10 E. Schneble, G. T. Clifton, D. F. Hale and G. E. Peoples, *Methods Mol Biol*, 2016, **1403**, 797–817.
- 11 N. R. M. Reintjens, E. Tondini, A. R. de Jong, N. J. Meeuwenoord, F. Chiodo, E. Peterse, H. S. Overkleeft, D. V. Filippov, G. A. van der Marel, F. Ossendorp and J. D. C. Codee, *J. Med. Chem.*, 2020, **63**, 11691–11706.
- 12 D. M. McDonald, S. N. Byrne and R. J. Payne, *Front Chem*, 2015, **3**, 60.
- 13 M. E. Kirtland, D. C. Tsitoura, S. R. Durham and M. H. Shamji, *Front Immunol*, 2020, **11**, 599083.
- 14 S. Kumar, R. Sunagar and E. Gosselin, *Front Immunol*, 2019, **10**, 1144.
- 15 G. G. Zom, M. Willems, S. Khan, T. C. van der Sluis, J. W. Kleinovink, M. G. M. Camps, G. A. van der Marel, D. V. Filippov, C. J. M. Melief and F. Ossendorp, *J Immunother Cancer*, 2018, **6**, 146.
- 16 M. Zaman and I. Toth, *Front Immunol*, 2013, **4**, 318.
- 17 T. Aiga, Y. Manabe, K. Ito, T. C. Chang, K. Kabayama, S. Ohshima, Y. Kametani, A. Miura, H. Furukawa, H. Inaba, K. Matsuura and K. Fukase, *Angew Chem Int Ed Engl*, 2020, **59**, 17705–17711.
- 18 T. C. Chang, Y. Manabe, Y. Fujimoto, S. Ohshima, Y. Kametani, K. Kabayama, Y. Nimura, C. C. Lin and K. Fukase, *Angew Chem Int Ed Engl*, 2018, **57**, 8219–8224.



- 19 Z. Y. Sun, P. G. Chen, Y. F. Liu, B. D. Zhang, J. J. Wu, Y. X. Chen, Y. F. Zhao and Y. M. Li, *Chem Commun*, 2016, **52**, 7572–7575.
- 20 H. Cai, Z. Y. Sun, M. S. Chen, Y. F. Zhao, H. Kunz and Y. M. Li, *Angew Chem Int Ed Engl*, 2014, **53**, 1699–1703.
- 21 S. Krishna and K. S. Anderson, *Methods Mol Biol*, 2016, **1403**, 779–796.
- 22 S. Ingale, M. A. Wolfert, J. Gaekwad, T. Buskas and G. J. Boons, *Nat. Chem. Biol.*, 2007, **3**, 663–667.
- 23 B. L. Wilkinson, S. Day, L. R. Malins, V. Apostolopoulos and R. J. Payne, *Angew Chem Int Ed Engl*, 2011, **50**, 1635–1639.
- 24 H. Cai, Z. Y. Sun, Z. H. Huang, L. Shi, Y. F. Zhao, H. Kunz and Y. M. Li, *Chemistry*, 2013, **19**, 1962–1970.
- 25 M. Li, Z. Wang, B. Yan, X. Yin, Y. Zhao, F. Yu, M. Meng, Y. Liu and W. Zhao, *RSC Med. Chem.*, 2019, **10**, 2073–2077.
- 26 M. L. Visciano, M. Tagliamonte, M. L. Tornesello, F. M. Buonaguro and L. Buonaguro, *J Transl Med*, 2012, **10**, 4.
- 27 H. Cai, M. S. Chen, Z. Y. Sun, Y. F. Zhao, H. Kunz and Y. M. Li, *Angew Chem Int Ed Engl*, 2013, **52**, 6106–6110.
- 28 T. Chodon, R. C. Koya and K. Odunsi, *Immunol Invest*, 2015, **44**, 817–836.

